Excitation intensity and thickness dependent emission mechanism from an ultrathin InAs layer in GaAs matrix

Cite as: J. Appl. Phys. 124, 235303 (2018); https://doi.org/10.1063/1.5053412 Submitted: 22 August 2018 . Accepted: 29 November 2018 . Published Online: 18 December 2018

Rahul Kumar 🗓, Yurii Maidaniuk, Andrian Kuchuk 🗓, Samir K. Saha, Pijush K. Ghosh, Yuriy I. Mazur 🗓, Morgan E. Ware 📵, and Gregory J. Salamo







ARTICLES YOU MAY BE INTERESTED IN

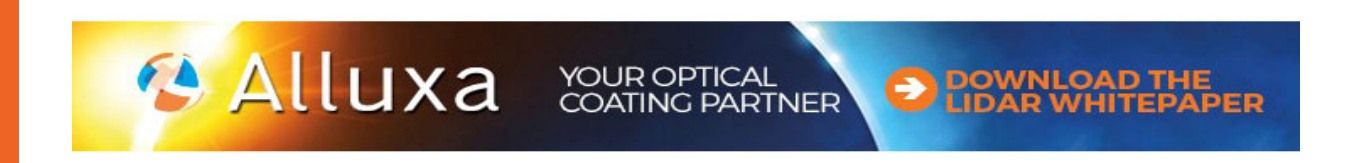
Enhanced ultraviolet emission from self-assembled ZnO nanorods grown on graphene Journal of Applied Physics 124, 235302 (2018); https://doi.org/10.1063/1.5064395

A predictive modeling study of the impact of chemical doping on the strength of a Ag/ZnO interface

Journal of Applied Physics 124, 235304 (2018); https://doi.org/10.1063/1.5051987

Atomic resolution of interface diffusing in short-period InAs/GaSb superlattice Journal of Applied Physics 124, 245301 (2018); https://doi.org/10.1063/1.5059350







Excitation intensity and thickness dependent emission mechanism from an ultrathin InAs layer in GaAs matrix

Rahul Kumar, ¹ Yurii Maidaniuk, ¹ Andrian Kuchuk, ¹ Samir K. Saha, ¹ Pijush K. Ghosh, ² Yuriy I. Mazur, ¹ Morgan E. Ware, ² and Gregory J. Salamo ¹

¹Institute for Nanoscience and Engineering, University of Arkansas, Fayetteville, Arkansas 72701, USA ²Department of Electrical Engineering, University of Arkansas, Fayetteville, Arkansas 72701, USA

(Received 22 August 2018; accepted 29 November 2018; published online 18 December 2018)

A set of samples containing a single ultrathin InAs layer with varying thickness from 0.5 to 1.4ML in a GaAs matrix have been grown by molecular beam epitaxy on GaAs (001) substrates at low temperatures and investigated by low-temperature photoluminescence (PL). A linear change in emission energy with InAs thickness has been experimentally observed. The PL emission line shape from InAs/GaAs heterostructures has been investigated as a function of incident optical intensity. The interplay between uncorrelated electron-hole pairs, free excitons, and localized excitons, as a function of the excitation intensity, is found to play a significant role on the optical properties of the InAs layer and is described in detail. *Published by AIP Publishing*. https://doi.org/10.1063/1.5053412

I. INTRODUCTION

Highly strained ultrathin InAs layers on GaAs have attracted much interest in the study of fundamental physics¹ as well as in applications for electronic and optoelectronic devices.^{2,3} For example, recently, sub-monolayer (SML) InAs deposition on GaAs⁴ has been proposed as an alternative method to the extensively used Stranski-Krastanow (SK) mode of quantum dot (QD) growth to achieve carrier confinement. Moreover, both theoretical⁵ and experimental⁶ investigations encourage the use of InAs single quantum wells (QWs) for efficient excitonic lasing applications. These investigations raise an interesting question as to the degree and role of carrier confinement in nanostructures formed by sub-monolayer growth.

For example, it has been reported that carriers confined to an ultrathin InAs layer show confinement in one dimension, and any restriction on center-of-mass motion of excitons in the lateral direction due to the InAs island nature can be excluded. This is in contrast to other works, which argue for a significant role for the lateral confinement by the island geometry. Consequently, the question of whether an exciton in an ultrathin InAs layer is free in-the-plane of the layer or if it experiences in-plane confinement due to the isolated nature of the island, or coupling between islands, is interesting to explore.

To explore this question, the focus of this paper is on the excitation intensity dependence of photoluminescence (PL) to investigate carrier recombination in different monolayer InAs structures ranging from 0.5ML to 1.4ML, embedded in a GaAs matrix. We observe and study the PL line just below the GaAs free exciton (FE) peak, which is very strong even though it is only on the order of a single ML of the material. This PL line is due to the recombination of an excited electron and heavy hole in InAs.⁴ A very intense PL emission line from a thin InAs quantum well compared to the GaAs barrier has also been reported in the literature.^{10–12} We demonstrate here that the PL intensity does not simply depend on

the thickness of the InAs layer but also on other factors. For example, at lower InAs thickness, appreciable carrier escape into the barrier has been observed, which decreases the PL intensity drastically. By investigating the intensity dependence of the PL on the InAs coverage, we demonstrate that there are different channels of radiative recombination and therefore the nature of carrier confinement.

II. EXPERIMENTAL PROCEDURE

Samples have been grown by the conventional Molecular Beam Epitaxy (MBE) on semi-insulating (SI) GaAs (001) substrates. After the oxide desorption, a 500 nm thick GaAs buffer layer is grown at 580 °C. Subsequently, the substrate temperature has been brought down to 460 °C. At this substrate temperature and relatively higher As₄ overpressure, five different thicknesses of InAs (0.5, 0.75, 1, 1.2, and 1.4ML) have been grown on GaAs. A low substrate temperature and a high As₄ overpressure during InAs growth were used to minimize indium segregation. 13 Indium segregation and subsequent In/Ga intermixing have been studied in great detail for the III-V alloy system and for ML scale InAs. 14,15 After the deposition of InAs, a 10 s growth interruption was introduced to get rid of liquid like indium or clustering on the surface. After the InAs layer, a 5 nm layer of GaAs was grown at the same temperature to minimize In diffusion. The substrate temperature was then increased to 580 °C, and a 45 nm GaAs layer is grown. Reflection high energy electron diffraction (RHEED) was used to monitor the growth in real time. Throughout the growth, a streaky RHEED pattern indicated that we maintained two-dimensional growth.

After the growth, photoluminescence (PL) and X-ray diffraction (XRD) measurements were carried out on the samples. For low-temperature PL measurements, the samples were mounted in a closed-cycle cryostat (Janis CCS-150) with temperatures varying from 10 to 300 K and excited by a 532-nm continuous-wave (CW) laser. The PL signal was

detected by a liquid nitrogen cooled CCD detector array (Princeton Instruments PyLoN: 1024-1.7) attached to a 50-cm focal-length spectrometer (Acton 2500). All of the PL spectra presented in this paper have been measured at 10 K. XRD scans were performed on a PANalytical X'Pert MRD diffractometer equipped with a multilayer focusing mirror, a standard four-bounce Ge (220) monochromator providing a collimated and monochromatic incident Cu K α 1 source of radiation (λ = 0.15406 nm), and a Pixel detector. In this case, ω -2 θ scans, measured in the vicinity of GaAs (004) reflection, were used for the characterization of the layer's thickness and strain.

III. CHARACTERIZATION OF SUB-MONOLAYER INAS SAMPLES

A. X-ray diffraction (XRD)

Interference of the X-ray wave field in the semiconductor heterostructure was used to analyze the structural properties of the ultrathin layers. 16 The interference from x-rays scattered from GaAs below the InAs layer and the GaAs cap layer was observed in the XRD pattern as the pendellösung fringes. This allowed us to confirm the total deposited indium, which was calibrated with RHEED, by comparing the XRD measurement with dynamical scattering theory simulations. 17 This technique provides accuracy better than 0.1ML.¹⁸ Figure 1 shows the symmetrical (004) XRD pattern (both experimental and simulated) of the samples under consideration. Excellent agreement between experimental and simulated curves can be observed. Simulation has been performed considering a fully strained system. Calculated "effective thickness of the InAs layer" from curve fitting has been tabulated in Fig. 1. The samples have been named on the basis of InAs coverage, for example, a sample having an

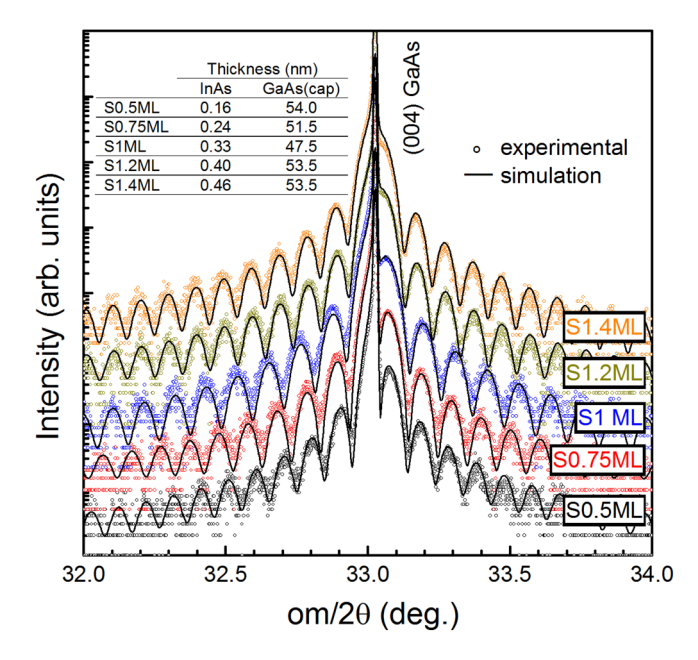


FIG. 1. XRD determined the effective or average thickness of the InAs material. Experimental (symbols) and simulated (black solid lines) XRD pattern for the symmetrical (004) plane; the table in the inset shows the calculated thickness of GaAs and InAs layers.

average InAs layer thickness of 0.5ML has been named S0.5ML. It is important to note that the thickness determined by x-ray simulation agrees exceptionally well with the intended ML deposition based on the growth rate determined by RHEED oscillations. It should also be noted that the effective thickness of the well due to In/Ga intermixing will result in a thicker InGaAs layer.

B. Photoluminescence (PL)

Before discussing the excitation intensity dependence of PL, we discuss some general features of the observed PL to characterize the emission. For example, Fig. 2(a) shows the low-temperature PL spectra of the ultrathin InAs samples at a low excitation power. It allows us to observe the distinct PL line shapes of all samples. A few simple observations from the PL spectra are as follows: PL emission energy of InAs heavy hole (hh) exciton line decreases linearly as the deposition of InAs, from 0.5ML to 1.4ML, increases [Figs. 2(a) and 2(b)]; Full width at half maximum (FWHM) of the InAs hh exciton line increases with InAs deposition, except for the 1ML sample, which falls out-of-step and is relatively narrow [Figs. 2(a) and 2(b)]; InAs hh exciton line is asymmetric in nature with a low-energy-tail for all samples, except, again, for the 1ML sample, which is very symmetric [Fig. 2(a)].

The PL emission energy, as a function of deposition, for the InAs hh-line is plotted in Fig. 2(b). The decrease in the emission peak energy with the InAs thickness is approximately linear. A similar trend was observed in the earlier reports of thin InAs layers in GaAs. 11,12 If InAs submonolayers were simply composed of ML high InAs islands, one could expect to see a PL characteristic of 1ML for all of them. Likewise, for a deposition between 1ML and 2ML, one would expect to observe PL for both 1ML and 2ML quantum wells. However, this is not observed, rather the observed PL peak behaves roughly linearly with deposition from 0.5ML to 1.4ML.

An explanation for the linear, as opposed to the discrete change in the PL peak with deposition, is that previous studies on less than 1ML InAs islands show that the in-plane island size is on the order of 2 to 4 nm.^{7,17,19} This is much smaller than the exciton Bohr radius $(a_B \approx 15 \text{ nm})^7$, and therefore there can be carrier confinement and sharing of the carrier wavefunction with the barrier or other islands. In this case, either due to lateral confinement or coupling between islands, we need not observe the same PL peak energy for S0.5ML and S0.75ML, or discrete PL peak energies for 1ML and 2ML quantum wells for S1.2ML and S1.4ML, 17 but instead we can understand a more gradual change in the PL emission peak energy with the amount of InAs deposited. Likewise, another explanation for this PL behavior can be based on intermixing of In and Ga from already formed InAs islands during GaAs capping, which results in In_xGa_{1-x}As islands in which case the peak PL energy can shift more gradually due to a changing value of "x" with increasing deposition time. Our data for the shift in peak PL energy do not distinguish between the two possibilities.

The PL linewidth, as a function of deposition, of the InAs hh-line is plotted in Fig. 2(b). The increase in the

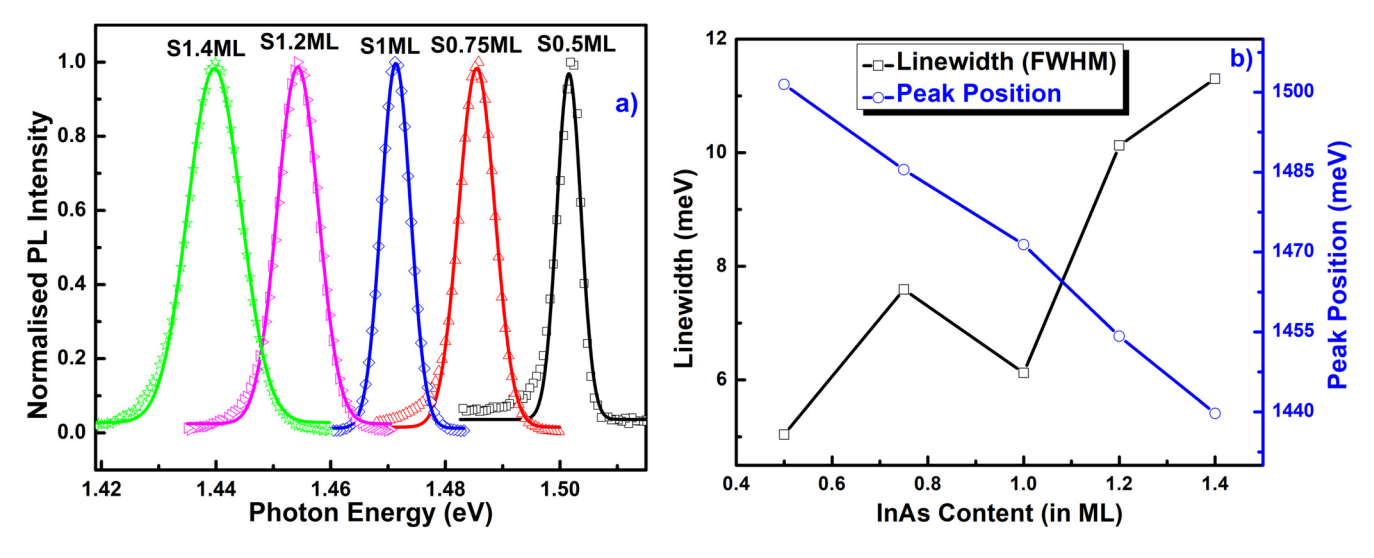


FIG. 2. (a) Low temperature (10 K) normalized PL spectra of InAs samples (measured data plotted by symbols) and Gaussian fitting of InAs PL peak demonstrate the asymmetry toward low energy side (Gaussian fitted data are plotted by solid lines). (b) Variation of PL peak energy and linewidth (FWHM) with InAs content.

emission linewidth or FWHM with the InAs thickness is gradual, except at S1ML. The most likely and the most cited explanation for this is based on the research by Singh *et al.* who examined an exciton in an island when the lateral extent of those islands is smaller than the exciton Bohr radius using

the virtual crystal approximation (VCA) model.²⁰ Applying these results to our case, the spectral broadening of the PL emission line²¹ can be due to interface roughness.^{17,19} A second possibility is related to island nucleation. Increased deposition simply means that while already existing islands

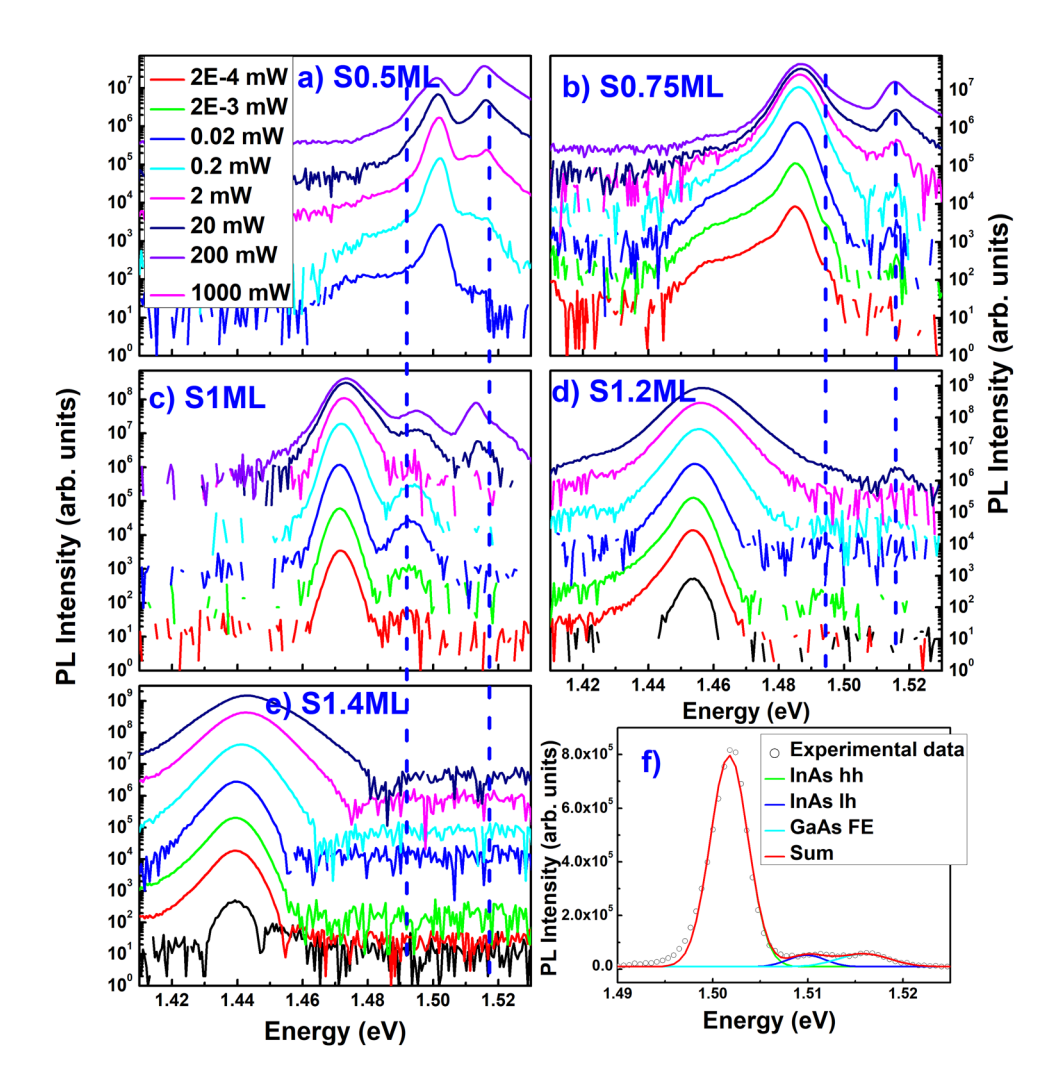


FIG. 3. (a)–(e) Excitation power dependent PL spectra of all samples; two dashed blue lines show the approximate position of GaAs related peaks and (f) de-convolved PL spectra of S0.5ML.

are ripening, new ones are nucleating, causing the island distribution to broaden.²² A third possibility is that In/Ga intermixing, from already formed InAs islands during GaAs capping, results in material inhomogeneity that broadens the emission. In either case, the narrow linewidth for the S1ML InAs is understandable since for near 1ML of InAs coverage, the roughness is reduced, the InAs island size distribution is a much smaller issue, and intermixing is only vertical.

PL spectra of all samples [Fig. 2(a)], except sample S1ML, show an asymmetric peak shape under low power excitation in which the low energy side has an extended tail, especially for S0.5ML and S0.75ML, as observed in the poor Gaussian fit in Fig. 2(a). One explanation for the asymmetric PL line shape is the carrier localization in the lower energy states.²³ A tail of localized excitonic states appears for a noninteger amount of InAs, possibly due to increased roughness. Gradual fading of the low-energy-tail as the excitation power is increased (see Fig. 3) can be explained by the filling of these localized exciton states because of their finite density. Another possible explanation is that the tail is due to interface or island edge states below the conduction band. The tail is also observed to be minimized for S1ML and to decrease for all samples relative to the PL peak as the excitation power is increased (see Fig. 3). This is consistent with the relative increase in free excitons or the saturation of the edge states with increased excitation intensity.

While these three observations are consistent with previous experiments, here we have observed that the incident excitation intensity has a significant effect on the PL emission peak, FWHM, and asymmetry. This presents an opportunity to learn more about the relationship between the InAs coverage and the corresponding PL. As a result, the PL spectra were measured with over 6 orders of magnitude variation in I_{exc} . The results are shown in Figs. 3(a)-3(e). Along with the InAs PL peak, the GaAs free-exciton peak (around 1.516 eV) and an impurity peak (around 1.495 eV) are observed. For the S0.5ML sample, in addition to InAs hh peak, a light hole (lh) related emission is also observed. The appearance of the lh related emission for the lower coverage of InAs is also found in previous reports. In Fig. 3(f), the hh, lh, and GaAs FE peaks are de-convolved for sample S0.5ML.

Our observations of the intensity dependent spectra are as follows: (1) the linewidth increases with excitation power; (2) in general, the PL peak blue-shifts with excitation power; (3) the intensity of the PL peak increases with excitation power; and (4) in general, the low energy tail observed for low power excitation vanishes with increasing excitation power.

In order to understand these results, the dependence of the PL linewidth, peak position, and integrated intensity on I_{exc} is investigated and each is summarized in Figs. 4 and 5.

Both the PL linewidth and peak position variation of the InAs hh peak with excitation power are plotted in Fig. 4. In addition to the five InAs thin layer samples, two samples having 1ML of In_{0.5}Ga_{0.5}As (S0.5InGaAs) and 1ML of In_{0.75}Ga_{0.25}As (S0.75InGaAs) sandwiched in the GaAs matrix have also been plotted in order to compare with the S0.5 ML and S0.75ML samples. In general, the observed trend can be characterized as a (1) blue shift and an (2) increase in

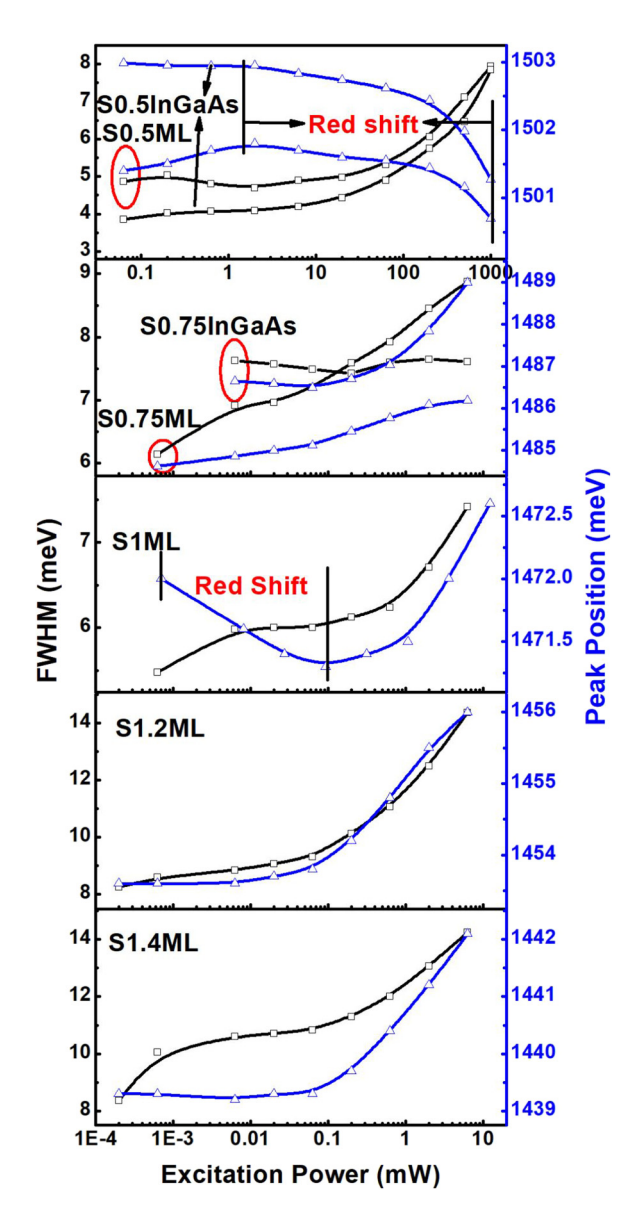


FIG. 4. Peak position and linewidth variation with excitation power. Blue lines and triangles show the peak position, whereas black lines and squares represent the FWHM.

linewidth with increasing I_{exc} . The general blue shift behavior can be attributed to carrier concentration dependent band filling with increasing I_{exc} (dynamic Burstein-Moss effect). I_{exc} increases the non-equilibrium carriers (n), which fills the states near the band edge, shifting the PL peak toward higher energy. As a result, competition between increasing n and the rate of recombination raises the quasi-Fermi level producing both an increase in linewidth and emission energy of the PL peak.

However, two anomalous behaviors of the I_{exc} dependent variation of the emission energy are also observed: (1) a redshift in the PL peak of sample S1ML at low I_{exc} followed by a blue shift of Pl peak at high I_{exc} and (2) a red-shift in the emission energy of sample S0.5ML and similar for S0.5InGaAs at high I_{exc} . The red-shift in S1ML (and a less pronounced red shift in 1ML InGaAs samples) at low I_{exc} can be understood in terms of competition between the formation of the free exciton (FE) and uncorrelated e-h pairs.

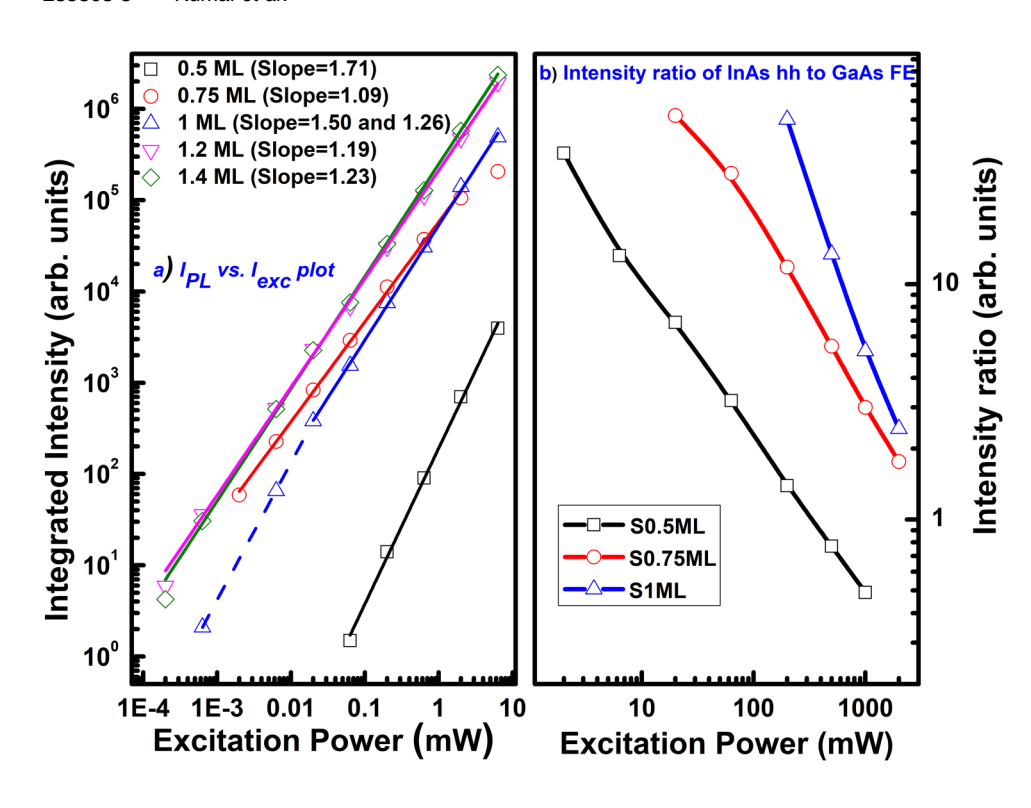


FIG. 5. (a) Variation of the integrated intensity of InAs hh peak with excitation power; all graphs fitted according to the power law mentioned in the text and the calculated exponent (α , written as slope) are shown in the figure. Error in the calculation of slopes is less than 0.05. (b) Variation of the intensity ratio between InAs hh peak and GaAs FE peak.

Exciton formation in the case of non-resonant excitation is most efficient at intermediate I_{exc} . At low temperatures and low I_{exc} , the probability for electron-hole collisions is small²⁴ and uncorrelated e-h pairs can affect the emission energy of PL peak. At low I_{exc} , uncorrelated e-h pair will influence the PL peak, while with an increase of I_{exc} , the effect of uncorrelated e-h pair will become insignificant. This assumption is further supported by the change in the slope of integrated intensity vs I_{exc} for S1ML, which will be discussed later. In other samples, instead uncorrelated e-h pairs at low excitation power localized excitons (LE) form due to the presence of localized states (consistent with our discussion of the PL peak having a low energy tail at low I_{exc}) and consequently, we do not observe a red-shift. Figure 4 shows the two different regions for the S1ML sample in I_{exc} vs. emission energy curve.

The red-shift in the emission energy in S0.5ML at high I_{exc} can be attributed to two mutually supportive processes: local heating effect and corresponding carrier escape from the InAs to GaAs barrier (due to small escape barrier potential). Carriers in the confined region have a higher radiative recombination efficiency than in the barrier where an exciton can find non-radiative recombination sites. Moreover, non-radiative recombination in the GaAs increases the lattice temperature, which in turn increases the carrier escape from the InAs to GaAs barrier. Hence, these two processes are multiplicative in nature. Local lattice heating is evident in samples S0.5ML, S0.75ML, and S1ML by carefully observing the red shift in GaAs FE emission. In our data, the red shift in the InAs PL peak is only observed in S0.5ML, probably because the escape probability of carriers from InAs to GaAs barrier in S0.5ML is highest among all samples.

For the integrated PL, Fig. 5(a) shows the PL behavior vs. I_{exc} . Basically, the integrated PL (I_{PL}) increases with increasing I_{exc} , based on the relation of $I_{PL} = \eta I_{exc}^{\alpha}$. The

exponent (α) gives information on the radiative recombination mechanism. For excitonic recombination, we expect that I_{PL} varies linearly with I_{exc} ($\alpha = 1$), while for uncorrelated electron-hole pairs recombination, I_{PL} is proportional to the square of I_{exc} ($\alpha = 2$). After fitting the experimental data, we find the exponent (α) for all samples to be near to unity except for S0.5ML. It shows that a strong radiative recombination mechanism is due to correlated e-h pairs with a significant fraction from uncorrelated e-h pairs. At the same time, I_{PL} of S0.5ML is almost 3 orders of magnitude lower than all other samples for the same value of I_{exc} . Considering the very small escape barrier height in the case of S0.5ML sample, carriers will escape as excitons, become uncorrelated, or escape as uncorrelated pairs. These carriers are easily lost to the GaAs barrier resulting in the drop of PL intensity. It was shown by Le Ru et al. that escape of the carrier modifies the dependence of I_{PL} on I_{exc} and makes it superlinear.²⁷ In the case of S0.5ML sample, relatively high exponent ($\alpha = 1.71$) is due to the carrier escape from the InAs to GaAs barrier. As expected, almost the same order of intensity and exponent is observed for the S0.5InGaAs $(1ML In_{0.5}Ga_{0.5}As)$ sample.

Earlier, we proposed that the interplay between FE and uncorrelated e-h pairs is the reason for the red-shift of PL peak in the S1ML sample at low I_{exc} . To examine the interplay between FE and uncorrelated e-h pair in the S1ML sample, I_{PL} variation of InAs hh peak with I_{exc} is divided into two regions, denoted by dashed and solid blue lines in Fig. 5(a). The low I_{exc} region is shown by a dashed line, where we observed the red shift in the emission energy, and the high I_{exc} region is shown by a solid line, where we observed the blue shift due to the band filling effect, as described earlier. Two distinct exponents (α) can be observed in these two regions. The low I_{exc} region shows the slope as high as 1.5 indicating the influence of uncorrelated e-h pair recombination in this

region. The high I_{exc} region shows the slope almost the same as other samples indicating that the main recombination channel in this region is FE recombination.

Under the specified laser illumination, carriers will be initially generated at an energy higher than the GaAs barrier and fall to the conduction and valence band edges of both the islands and the barrier. Therefore, here, we assume that approximately the same amount of carriers will be generated in all samples under the same excitation power and diffuse to the InAs. Higher ML InAs samples should capture more carriers because of the deeper ground state, larger size, and therefore larger capture cross section. 28 Figure 5(b) shows the intensity ratio of InAs hh to GaAs FE peak variation as a function of I_{exc} . The higher amount of InAs samples shows a higher intensity ratio supporting the assumption that the carrier capture is more efficient in larger ML InAs samples. At high I_{exc} , as expected, the integrated intensity of InAs peak for higher ML sample is higher. However, at low I_{exc} , the behavior is non-trivial. PL intensity from InAs will depend on the carrier capture efficiency of the InAs region, oscillator strength of carriers in the confined InAs region, and carrier escape from the InAs to GaAs barrier. Using these three factors, we can examine the integrated PL intensity behavior with I_{exc} . In general, one may expect the InAs PL intensity to increase with increasing InAs deposition. However, one has to also consider the escape and emission probability of carriers which are expected to be different for each sample. The observation that the InAs PL intensity is higher for S0.75 ML than S1ML is consistent with the expectation that the oscillator strength of correlated versus uncorrelated e-h pair is larger. Carriers in the S1ML sample are less correlated than the S0.75ML sample at low I_{exc} . Similarly, the higher PL intensity from the S1.2ML sample than the S1.4ML sample at low I_{exc} can be explained based on the exciton oscillator strength. With the increase in I_{exc} , localized states saturate and we observe the crossover [Fig. 5(a)] of integrated intensity between these samples.

IV. CONCLUSIONS

Different ML InAs (0.5 to 1.4ML) samples are grown on GaAs by MBE and their PL properties are investigated. Observed PL can be explained by either the island nature of InAs or InGaAs formation due to In and Ga intermixing. We do not distinguish between these two possibilities in our explanations and both may play a role. PL emission energy of the InAs heavy hole (hh) exciton line decreases linearly as the deposition of InAs, from 0.5ML to 1.4ML, increases: indium lateral intermixing, lateral confinement of carriers, and wavefunction spread over multiple InAs islands are possible explanations. Full width at half maximum (FWHM) of the InAs hh exciton line increases with InAs deposition, except for the 1ML sample, which falls out-of-step and is relatively narrow: interface roughness, island distribution broadening with increased coverage, and inhomogeneity introduced by intermixing are the possible reasons for linewidth broadening. The InAs hh exciton line is asymmetric in nature with a low-energy-tail for all samples, except, again, for the 1ML sample, which is very symmetric: increased roughness induced localized states or interface or edge state introduced localized states are possible origins of this low-energy-tail. In addition to the general behavior of the InAs PL, the excitation intensity dependent optical properties of ultrathin InAs in the GaAs matrix have been investigated to add to our understanding of the PL behavior. Red-shift of PL peak for 1ML InAs can be understood as the interplay of free exciton and uncorrelated electron-hole pairs. This assumption is supported by the two different slopes for the integrated PL intensity with excitation intensity. Red-shift of PL peak for 0.5ML InAs can be understood as local heating and carrier escape to the barrier. This is also consistent with the observed almost 3 orders of lower intensity for 0.5ML InAs. Nontrivial integrated PL intensity behavior of these samples has been explained by the interplay between different radiative recombination mechanisms, namely, uncorrelated e-h pair recombination, and localized and free excitonic recombinations.

ACKNOWLEDGMENTS

The authors acknowledge the financial support by the Institute of Nanoscale Science and Engineering, University of Arkansas, and the National Science Foundation (NSF) (Grant No. 1809054).

- ¹J. Brübach, A. Y. Silov, J. E. M. Haverkort, W. van der Vleuten, and J. H. Wolter, Superlattices Microstruct. **21**, 527 (1997).
- ²J. O. Kim, S. Sengupta, A. V. Barve, Y. D. Sharma, S. Adhikary, S. J. Lee, S. K. Noh, M. S. Allen, J. W. Allen, S. Chakrabarti, and S. Krishna, Appl. Phys. Lett. **102**, 11131 (2013).
- ³N. S. Beattie, P. See, G. Zoppi, P. M. Ushasree, M. Duchamp, I. Farrer, D. A. Ritchie, and S. Tomić, ACS Photonics 4, 2745 (2017).
- ⁴I. L. Krestnikov, N. N. Ledentsov, A. Hoffmann, and D. Bimberg, Phys. Status Solidi **183**, 207 (2001).
- ⁵R. C. Iotti, L. C. Andreani, and M. Di Ventra, Phys. Rev. B **57**, R15072 (1998).
- ⁶A. R. Goñi, M. Stroh, C. Thomsen, F. Heinrichsdorff, V. Türck, A. Krost, and D. Bimberg, Appl. Phys. Lett. **72**, 1433 (1998).
- ⁷Z. L. Yuan, Z. Y. Xu, B. Z. Zheng, J. Z. Xu, S. S. Li, W. Ge, Y. Wang, J. Wang, L. L. Chang, P. D. Wang, C. M. Sotomayor Torres, and N. N. Ledentsov, Phys. Rev. B **54**, 16919 (1996).
- ⁸M. V. Belousov, N. N. Ledentsov, M. V. Maximov, P. D. Wang, I. N. Yasievich, N. N. Faleev, I. A. Kozin, V. M. Ustinov, P. S. Kop'ev, and C. M. Sotomayor Torres, Phys. Rev. B 51, 14346 (1995).
- ⁹P. D. Wang, N. N. Ledentsov, C. M. Sotomayor Torres, I. N. Yassievich, A. Pakhomov, A. Y. Egovov, P. S. Kop'ev, and V. M. Ustinov, Phys. Rev. B **50**, 1604 (1994).
- ¹⁰M. A. Tischler, N. G. Anderson, and S. M. Bedair, Appl. Phys. Lett. 49, 1199 (1986).
- ¹¹K. Taira, H. Kawai, I. Hase, K. Kaneko, and N. Watanabe, Appl. Phys. Lett. **53**, 495 (1988).
- ¹²J. M. Gerard and J. Y. Marzin, Appl. Phys. Lett. **53**, 568 (1988).
- K. Muraki, S. Fukatsu, Y. Shiraki, and R. Ito, Appl. Phys. Lett. 61, 557 (1992).
 J.-M. Gérard, C. d'Anterroches, and J.-Y. Marzin, J. Cryst. Growth 127, 536 (1993).
- ¹⁵J. M. Moison, F. Houzay, F. Barthe, J. M. Gérard, B. Jusserand, J. Massies, and F. S. Turco-Sandroff, J. Cryst. Growth 111, 141 (1991).
- ¹⁶O. Brandt, L. Tapfer, R. Cingolani, K. Ploog, M. Hohenstein, and F. Phillipp, Phys. Rev. B 41, 12599 (1990).
- ¹⁷C. A. Tran, R. A. Ares, V. A. Karasyuk, S. P. Watkins, G. Letourneau, and R. Leonelli, Phys. Rev. B 55, 4633 (1997).
- ¹⁸C. Giannini, L. Tapfer, S. Lagomarsino, J. C. Boulliard, A. Taccoen, B. Capelle, M. Ilg, O. Brandt, and K. H. Ploog, Phys. Rev. B 48, 11496 (1993).
- ¹⁹A. Patanè, A. Polimeni, M. Capizzi, and F. Martelli, Phys. Rev. B 52, 2784 (1995).
- ²⁰J. Singh, K. K. Bajaj, and S. Chaudhuri, Appl. Phys. Lett. **44**, 805 (1984).

- ²¹J. Christen and D. Bimberg, Phys. Rev. B **42**, 7213 (1990).
- ²²Q. Jiang and G.-C. Wang, Surf. Sci. **324**, 357 (1995).
 ²³R. Grousson, V. Voliotis, N. Grandjean, J. Massies, M. Leroux, and C. Deparis, Phys. Rev. B **55**, 5253 (1997).

 ²⁴S. Chatterjee, C. Ell, S. Mosor, G. Khitrova, H. M. Gibbs, W. Hoyer,
- M. Kira, S. W. Koch, J. P. Prineas, and H. Stolz, Phys. Rev. Lett. 92, 67402 (2004).
- ²⁵S. Jin, Y. Zheng, and A. Li, J. Appl. Phys. **82**, 3870 (1998).
- ²⁶J. Fouquet and R. Burnham, IEEE J. Quantum Electron. **22**, 1799 (1986).
- ²⁷E. C. Le Ru, J. Fack, and R. Murray, Phys. Rev. B **67**, 245318 (2003).
- ²⁸Y. Wang, X. Sheng, Q. Guo, X. Li, S. Wang, G. Fu, Y. I. Mazur, Y. Maidaniuk, M. E. Ware, G. J. Salamo, B. Liang, and D. L. Huffaker, Nanoscale Res. Lett. 12, 229 (2017).